Nigerian Journal of Physics (NJP)
ISSN online: 3027-0936
ISSN print: 1595-0611
DOI: https://doi.org/10.62292/njp.v33i2.2024.222
Volume 33(2), June 2024

Statistical Tests of the Relativistic Beaming Indicators of jetted AGNs and Implication for the Revised Blazar Sequence

***[1]Iyida, E. U., [2]Onah, C. I. and [3]Eya, I. O.**

[1]Department of Physics and Astronomy, Faculty of Physical sciences, University of Nigeria
[2]Department of Physics and Astronomy, Federal University of Technology, Owerri, Nigeria
[3]Department of Science Laboratory Technology, Faculty of Physical sciences, University of Nigeria, Nsukka, Nigeria

*Corresponding author's email: uzochukwu.iyida@unn.edu.ng

ABSTRACT

The latest detection by the *Fermi* Large Area Telescope (*Fermi*-LAT) of strong relativistic jets of very high-energy (VHE, above 100 GeV) from the Narrow-Line Seyfert 1 Galaxies (NLS1s) has opened a new unified scheme of active galactic nuclei (AGN) in which jetted Seyfert galaxies are viewed as counterparts to a subclass of AGNs. In this paper, we report a systematic investigation of the revised blazar sequence using the γ-ray Doppler factor (δ_γ) and the radio core-dominance parameter (R) of AGN samples of NLS1s and blazar subtypes of flat-spectrum radio quasars (FSRQs) and BL Lac objects (BLs). Furthermore, we explore the γ-ray properties of NLS1s and blazar subtypes in the context of the blazar unification scheme at different scales. The main results are as follows: (a) The average values of R and γ-ray luminosity (L_γ) of our sample agree with the sequence BLs – FSRQs – NLS1s and provide quantitative explanations for the observed relativistic beaming effects in these objects. (b) Through a parameter t-test and non-parametric K-S test with chance probability $p < 10^{-3}$, we find that the distributions of R and L_γ for NLS1s and the blazar subtypes are not significantly different. (c) There is a regular positive trend ($r > +0.79$) in the variation of $L_\gamma - \delta_\gamma$ data from BLs to NLS1s through FSRQs which is consistent with the prediction of the revised blazar sequence. These results imply that NLS1s could fit very well into the conventional blazar sequence.

Keywords:
Data analysis
Gamma rays
General galaxies
Active galaxies
Jets.

INTRODUCTION

As an exceptional type of galaxy, the active galactic nuclei (AGNs) are well-known by the copious emissions which are fuelled by accreting supermassive black hole (SMBH). This happens mainly due to the presence of ultra-relativistic jets. AGNs are generally classified as radio-loud or radio-quiet, depending on the power of the radio emitting synchrotron jets. For the radio-loud AGNs, the jets are extremely relativistic and spread to long distances (up to megaparsec) which is more than the magnitude of the host galaxy. However, in radio-quiet type, the jets are within the host galaxy (Kellerman et. al. 1995). Blazars are few (>10 %) and the most extreme subtype of radio-loud AGNs whose relativistic jets are focused toward the line of sight of the observer (Urry and Padovani 1995). The emissions from these jets are highly boosted and dominant at every accessible wavelengths as a result of the effect of relativistic beaming (Sbarrato et al. 2014; Pei et al. 2020a).

Blazars include flat-spectrum radio quasars (FSRQs) and BL Lacertae objects (BLs) based on their optical emission properties. FSRQs have strong, quasar-like spectra with rich optical emissions while BLs have very weak and in most cases lack emission lines (Urry and Padovani, 1995; Giommi et al. 2012). In addition, the synchrotron peak frequency (ν_{peak}) of FSRQs is low and lies between 10^{12} - 10^{14} Hz while BLs have a long range of ν_{peak} leading to different subdivisions. These include: the low synchrotron peaked (LSPs) with $\nu_{peak} < 10^{14}$ Hz, intermediate synchrotron peaked (ISPs) with ν_{peak} from 10^{14} - 10^{15} Hz and high synchrotron peaked (HSPs) with $\nu_{peak} > 10^{15}$ Hz (Padovani and Giommi 1995; Fan et al. 2016; Ackermann et al. 2015; Acero et al. 2015). Detailed studies of AGNs in the MeV – GeV – TeV regimes using *Fermi* Large Area Telescope (*Fermi*-LAT) found that blazars are strong γ-ray emitters and

possess other outstanding characteristic properties such as rapid variability, high optical polarization and apparent superluminal motion in the inner radio jets (Bassani et al. 1983; Lister et al. 2013; Yang et al. 2019; Lu et al. 2019; Xiao et al. 2020; Fan et al. 2021)

Prior to the launch of *Fermi*-LAT, FSRQs, and BLs were the only well-studied subsets of radio-loud AGNs that were known to possess strong relativistic jets and emit in high-energy bands. However, the latest detection by *Fermi*-LAT of strong relativistic jets of very high-energy (VHE, above 100 GeV) from the Narrow-Line Seyfert 1 Galaxies (NLS1s) revealed the presence of another subclass of AGNs after blazars and radio galaxies (Abdo et al. 2009a, Abdo et al. 2009b; Komossa, 2018; Foschini, 2020). The study of the continuum emissions from NLS1s shows that they have remarkable properties across the electromagnetic spectrum such as substantial soft X-ray excesses, steep X-ray spectra, rapid variability, strong emissions from forbidden high-ionization lines, and relatively high luminosity (see, Stephens 1989; Pogge 2000).

According to the spectral energy distributions (SEDs) of jetted AGNs, the blazar unification scheme suggests that the different subtypes of blazars can be arranged in a sequence from HSPs to FSRQs through LSPs and ISPs in order of decrease in the synchrotron peak frequencies/energies and increase in source power, popularly known as *blazar sequence* (Fossati et al. 1997; 1998, Ghseillini et al. 1998; Ghisellini 2008; Mao et al. 2016; Ghisellini et al. 2017; Iyida et al. 2021). Originating in Fossati et al. (1998) and extended in subsequent works such as Ghisellini & Tavecchio (2008) and Ghisellini et al. (2017), the blazar sequence posits an inverse relationship between γ-ray luminosity and peak frequency of the low-energy synchrotron hump for γ-ray blazars. This blazar sequence has been extended different authors (Ghisellini & Tavecchio; 2008; Chen et al. 2015; 2021, Audu et al. 2023) who link the properties of the jet, and therefore the SED, with the black hole mass and accretion rate. This updated version called revised blazar sequence proposes that the jetted narrow line Seyfert 1 galaxies should be accommodated in the original blazar sequence. Although, the scientific community generally accepts this unification scheme, some astrophysicists intrigued by some results support the modification of the sequence (Foschini 2017; Berton et al. 2018; Chen and Gu 2019; Chen et al. 2021; Iyida et al. 2022b). These authors suggest that since NLS1s harbor powerful relativistic jet whose black hole mass is relatively small; they can be unified with the blazar subclasses. Some other authors opined that the γ-ray spectral indices of NLS1s have been observed to be similar to blazars (Abdo et al. 2009; Zhang et al. 2013; Paliya et al. 2013; Foschini et al. 2015; Sun et al. 2014, 2015). This is supported by the strong evidence that some well-known NLS1s such as RXJ 16290+4007 has been observed to display blazar-like properties such as rapid variability properties, emitting from radio up to the TeV γ-ray bands (Falcone et al. 2004; Schwope et al. 2000; Grupe et al. 2004). This forms the revised blazar sequence and it is intended to study how these blazar-like objects can embrace NLS1s as a third subclass of jetted AGNs that is observed under a different geometry.

Following this line of argument, we embark on the investigation of the connection between NLS1s and the normal blazar subtypes and how they can be accommodated in the blazar sequence. This forms the motivation for this research. In this paper, the relation between blazars and NLS1s is tested in the framework of blazar unified scheme using relativistic beaming phenomenon. This is done by statistically investigating their relativistic beaming properties to see whether or not they can be unified.

On relativistic beaming effect

The relativistic beaming model assumes that AGNs that are observed at an angle to the line of sight are associated with relativistically boosted emissions (Orr and Browne 1982). This relativistic theory has notably proven effective in clarifying the observational properties of jetted AGNs. The model involves studying the emission mechanisms from two luminosity components: the core and extended components (Orr and Brown, 1982; Fan and Zhang, 2003). The ratio of the two emission components called core-dominance parameter (R) is an essential statistical indicator of relativistic beaming and can be expressed as

$$R = \frac{\delta^{n+\alpha} S_C}{S_E} = \frac{R_T}{2}[(1-\beta\cos\varphi)^{-n+\alpha} + (1+\beta\cos\varphi)^{-n+\alpha}] \quad (1)$$

with S_C and S_E being intrinsic core and extended flux densities, α is the energy spectral index defined as $\boldsymbol{S_\nu \approx \nu^{\pm\alpha_\nu}}$, n = 2 for a continuous jet model, n = 3 for medium with blobs (Lind et al., 1985), φ is the angle between the jet and the line of sight, $R_T = R(\phi = 90^o)$ while $\delta$is the Doppler factor. The relativistic beaming effect is primarily described by this Doppler factor at very small observing angles (Bai and Lee, 2001; Nieppola et al. 2008; Meyer et al., 2011) and in this case, $\delta = \gamma^{-1}(1-\beta\cos\varphi)^{-1}$ where $\gamma = \left[(1-\beta^2)^{\frac{1}{2}}\right]^{-1}$ is the Lorentz factor. It can be deduced from equation (1) that the distribution of R and δcan give essential information about NLS1s, FSRQs and BLs in the context of unification scheme.

In the relativistic beaming paradigm, the luminosity (L) of a relativistic jet at observing frequency (ν) is given (Wu et al. 2009; Meyer et al. 2011) by:

$$L = L_0\delta^{n+\alpha}, \quad (2)$$

L_0 is the luminosity that would be measured by an observer in the frame of the radiating material. For γ-ray

emissions with flux density (S) and redshift (z), the luminosity can be rewritten as

$$L_\gamma = 4\pi\, d_L^2\, \frac{S}{(1+z)^{2-\Gamma\gamma}} \quad (3)$$

where Γ_γ is the photon spectral index and $\boldsymbol{d_L} = \boldsymbol{H_o^{-1}} \int_0^z [(\mathbf{1}+\boldsymbol{z})^2(\mathbf{1}+\boldsymbol{\Omega_m z}) - \boldsymbol{z}(\mathbf{2}+\boldsymbol{z})\boldsymbol{\Omega_\Lambda}]^{-\mathbf{1}/\mathbf{2}}\, \boldsymbol{dz}$is the luminosity distance. If the number of photons ($\mu_{(L_E \to H_E)}$) observed from low energyL_E to high energy H_E with values 1.00 and 100 GeV respectively is known, the total observed flux can be obtained using

$$S^{obs} = \mu_{(L_E \to H_E)} \frac{1-\Gamma\,(H_E^{2-\Gamma} - L_E^{2-\Gamma})}{2-\Gamma\,(L_E^{1-\Gamma} - L_E^{1-\Gamma})} \quad (4)$$

The Doppler factor is an important parameter that reveals the level of relativistic beaming effect and explain the observed extreme properties of jetted AGNs even though it is typically problematic to measure. It is usually assumed in SED modelling that the γ-ray emission is produced closer to the supermassive black hole than the radio core of the jet where most of the radio emission originate. Relativistic beaming affects both the apparent intensity of emitted radiation (through Doppler boosting) and the likelihood of interactions between γ-rays and the surrounding material (which affects optical depth). Therefore, following Mattox *et al.* (1993) and on the premise of multi-wavelength emission components, the emission size $(R_{size}) = \frac{c\delta\Delta}{(1+z)}$of jetted AGNs is controlled by the timescale variability, ΔT. Assuming that the emission region from the jets of AGNs is continuous, the γ-ray optical depth can be expressed as

$$\tau = 2 \times 10^3 \left[\frac{(1+z)}{\delta_\gamma}\right]^{(4+2\alpha)} \left(1 + z - \sqrt{1+z}\right)^2 h_{75}^{-2} \Delta T_5^{-1} \times \frac{S(keV)}{\mu Jy}\left(\frac{E_\gamma}{GeV}\right)^{\alpha} \quad (5)$$

where δ_γ is γ-ray Doppler factor, $h_{75} = \frac{H_0}{75}$, $\Delta T_5 = \frac{\Delta T}{10^5 s}$ is the timescale variability, S (ke$V$) and E_γ are flux at 1.00 keV and the energy at which the γ-rays are emitted respectively. Thus, by accounting for optical depth, one can refine models of relativistic jets of sources exhibiting relativistic beaming and this can enhance our understanding of phenomena like unification scheme for blazars and NLS1 galaxies. Adopting the timescale variability $\Delta T = 1$ day (24 hours) which has been consistent with previous results (Nalewajko 2013; Kang et al. 2014; Zhang et al. 2015) the γ-ray Doppler factor can be computed using

$$\delta_\gamma \approx \left[1.54 \times 10^{-3}(1+z)^{(4+2\alpha)} \left(\frac{d_L}{Mpc}\right)^2 \left(\frac{\Delta T}{h}\right)^{-1} \times \frac{S(keV)}{\mu Jy}\left(\frac{E_\gamma}{GeV}\right)^{\alpha}\right]^{\frac{1}{4+2\alpha}} \quad (6)$$

This γ-ray Doppler factor is found to correlate with the flux density which is a function of both luminosity and radio core-dominance parameter, implying that the jet is continuous in the γ-ray band and radio core-dominance parameter is an indicator of relativistic beaming. Therefore, the use of γ-ray Doppler factor is reasonable and substantial to explore the typical characteristic features of NLSIs and the blazar subclasses

MATERIALS AND METHODS

Sample Selection

One of the major challenges in the research of jetted AGNs is the completeness of the source parameters. So, in order to investigate the nature of the revised blazar sequence, we require a complete sample of blazars with a well-sampled SED such that a reliable relativistic beaming property can be obtained. However, as with many flux-limited samples in the history of extragalactic astronomy, there is a real possibility of observational biases against certain types of sources. Some recent arguments suggest that the phenomenon of the blazar sequence are purely selection effects (Giommi et al. 2012; Giommi & Padovani 2015) leading to sample biases. It is believed that our sample consistent of very brightest sources with γ-ray emission produced closer to the supermassive black hole than the outer radio cores of the jet. So, we assemble a large sample of *Fermi*-LAT blazars from the fourth catalogue with clear optical properties. First, we considered 507 blazars (comprising 263 FSRQs, 52 ISPs, 104 HSPs and 88 LSPs) and selected radio core dominance parameter, redshift and γ-ray Doppler factor from the Table 1 of Pei et al (2020a). Generally, radio observation is done at different frequencies as recorded by many authors. However, most of these data samples were not observed at a frequency of 5 GHz but they were converted to common frequency of 5 GHz using the relation given (Fan et al 2011; Pei et al. 2019; 2020a) as

$$S_C^{5GHz} = S_C^{\nu,obs} \text{ and } S_E^{5GHz} = S_E^{\nu,obs}\left(\frac{\nu}{5GHz}\right)^{\alpha_E} \quad (7)$$

where $\nu_{,\text{obs}}$ is the observed frequency

For the NLS1s sample, Foschini et al (2021) compiled a list of bonafide γ- ray emitting jetted AGNs (4 Seyfert galaxies and 12 NLS1s) with some parameters of interest. These objects were cross-matched with a compilation by Chen et al. (2021). We discovered that some of the sources do not overlap with the data from Foschini et al (2021) and hence, do not have complete data of the parameters of interest. However, these few samples of NLS1s did not affect our result. Throughout the paper, the standard cold dark matter (Λ-CDM) cosmology parameters: H_0 = 71.50 km/s/Mpc, Ω_Λ = 0.72, and Ω_m = 0.28 were adopted. All relevant data were adjusted in line with modern concordance cosmology

RESULTS AND DISCUSSION

We discuss in this subsection, the statistical comparison, distributions and correlation of the of relativistic beaming indicators of FSRQs, BL Lacs and NLSIs. We

analysed these distributions in order to understand the relationships of these sources in the framework of the blazar unification scheme. This is done using statistical tools such as the parameter *t*-test and the non-parametric, two-dimensional Kolmogorov–Smirnov (K-S) test. The *t*-test is used to check whether there is any difference in the mean values of the parameters of the subsamples while the K-S test is used to examine any difference in the distribution of the subsamples.

Distributions of Relevant Parameters

The distribution of the logarithm of γ-ray Doppler factor (δ_γ) of FSRQs was compared with that of BLs and NLS1s as shown in Fig. 1a. The γ-ray Doppler factor of FSRQs covers an interval of $10^{0.01}$ to $10^{1.41}$ with an average of $10^{0.8 \pm 0.20}$ whereas for the BLs, LSPs range from $10^{0.0}$ to $10^{1.62}$ with average of $10^{0.57 \pm 0.10}$, $10^{0.0}$ to $10^{1.62}$ with average of $10^{0.52 \pm 0.30}$ for ISPs, HSPs range from $10^{0.0}$ to $10^{1.48}$ with average value of $10^{0.47 \pm 0.10}$ while NLS1s range from $10^{0.02}$ to $10^{1.12}$ with average of $10^{0.41 \pm 0.20}$ at 95 % confidence level. Apparently, the distribution is clearly continuous for NLS1s, FSRQs and BLs. We performed *t*-test and K-S test with a 5 % significance level (chance probability value $p < 0.05$) on NLS1s, FSRQs and BLs data. The cumulative distribution function (CDF) is shown in Fig. 1b whereas the result is shown in Table 1. In the table, column (1) is the parameter that is used for the *K-S* test, column (2) gives NLS1s and the blazar subclass, column (3) gives the sample size (*n*) of NLS1s while column (4) gives that of the blazar subclass, column (5) is distance between the cumulative probabilities of the NLS1s and blazar subclass in the *K-S* test and column (6) gives the probabilities for NLS1s and blazar subclasses to come from the same parent population in the distribution. From the figure, we observed that there is less overlap in the values of γ-ray Doppler factor between NLS1s and blazar subclasses. This is an indication that there are over 95 % confidence that there is fundamental difference in the distribution of the objects in the γ-ray Doppler factor.

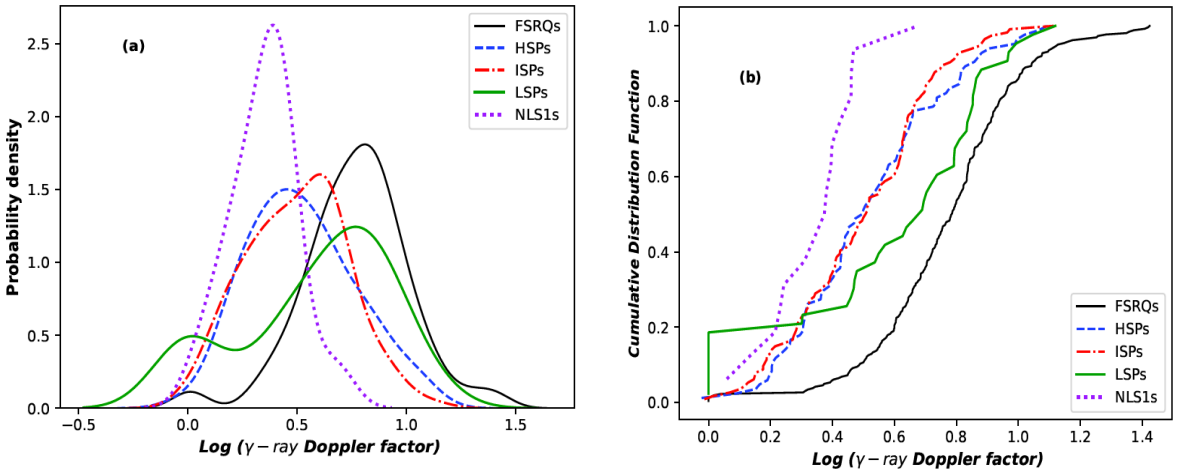

Figure 1: The density distribution of (a) γ-ray Doppler factor (b) cumulative distribution function of NLS1s, RQs and BLs

We also show the density distribution of γ-ray luminosity (erg s^{-1}) of NLS1s, FSRQs and BLs in Fig. 2a. The distribution is equally continuous with BLs displaced to lower values of γ-ray luminosity, NLS1s appear to have the highest values while FSRQs overlaps with up to 4 orders of magnitude. This suggests that NLS1s are strongest γ-ray emitters of FSRQs and BLs. We calculated the average values of γ-ray luminosity of NLS1s, FSRQs and BLs and obtained $10^{45.40 \pm 0.20}$ for FSRQs, $10^{45.10 \pm 0.30}$ for LSPs, $10^{44.20 \pm 0.10}$ for ISPs, $10^{44.10 \pm 0.20}$ for HSPs and $10^{47.50 \pm 0.20}$ for NLS1s. We discovered that the distribution of γ-ray luminosity agrees with the sequence, BLs – FSRQs – NLS1s. This sequence provides a quantitative explanation for the observed relativistic beaming effects in NLS1s, FSRQs and BLs which is consistent with the prediction of the revised blazar sequence. Furthermore, a *t*-test and K-S test carried out on the data indicate a zero chance probability as shown in Table 1 at confidence level 95%). This indicates that there is any fundamental difference between the underlying distributions of these objects in γ-ray luminosity.

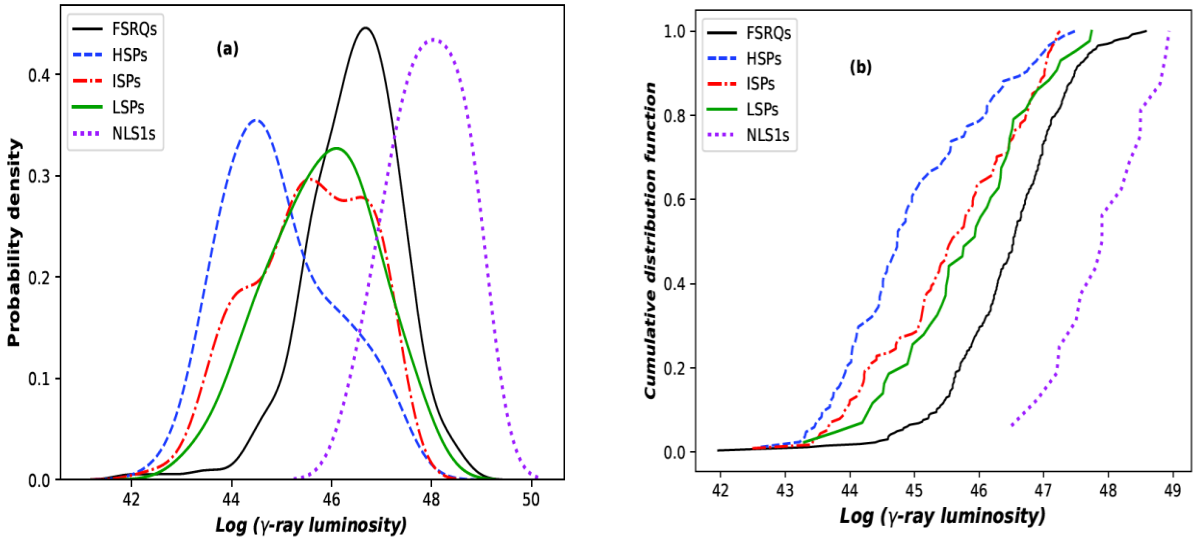

Figure 2: The density distribution of (a) γray luminosity (b) cumulative distribution function of NLS1s, FSRQs and BLs

The density distribution of radio core-dominance on logarithmic scale and the cumulative distribution function is shown in Figure 3a and 3b respectively. For FSRQs, the radio core-dominance parameter ranges from $10^{-1.9}$ to $10^{3.46}$ with average of $10^{0.60 \pm 0.10}$. In the case of BLs, LSPs range from $10^{-0.80}$ to $10^{3.12}$ with average of $10^{0.51\pm 0.20}$, $10^{-0.90}$ to $10^{3.40}$ with average of $10^{0.37\pm 0.30}$ for ISPs, HSPs range from $10^{-1.40}$ to $10^{3.90}$ with average value of $10^{0.23\pm 0.20}$ while NLS1s range from $10^{-0.08}$ to $10^{1.24}$ with average of $10^{0.86\pm 0.30}$ at 95 % confidence level. We found that the average values of NLS1s and FSRQs are higher than BLs within the possible measurement errors. This indicates the level of relativistic beaming effects in NLS1s and FSRQs. The parameter *t*-test performed on the subsamples shows that there is a significant difference between the average values of NLS1s and blazar subtypes of BLs and FSRQs ($p = 0.00023$). Similarly, a K-S test result shows that the distribution of the radio core-dominance parameter is not significantly different. Thus, the sequence of the sources is consistent with the revised blazar sequence via relativistic beaming.

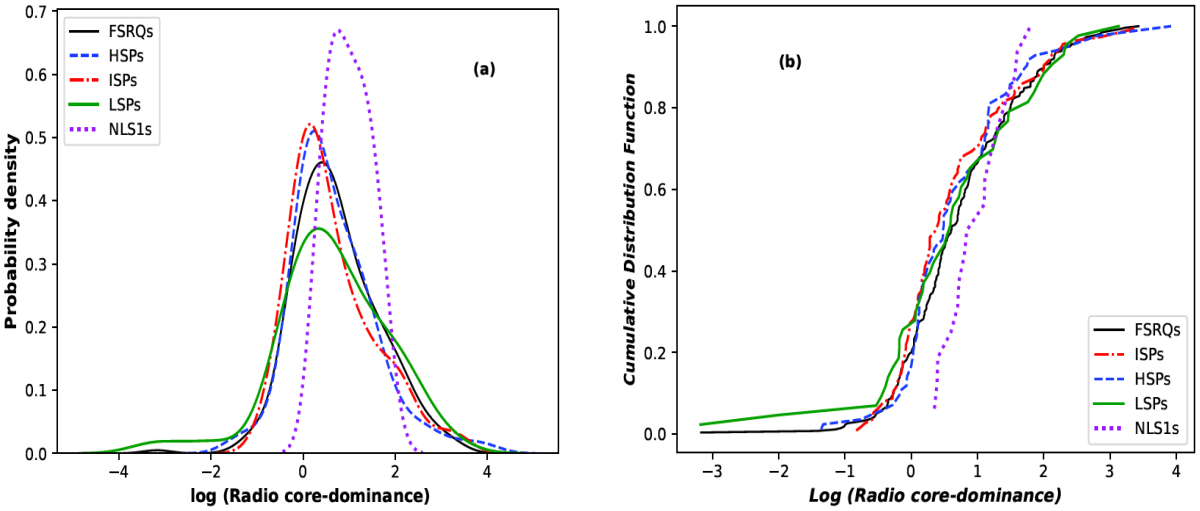

Figure 3: The density distribution of (a) radio core-dominance (b) cumulative distribution of NLS1s, FSRQs and BLs

To test further the consistency of the proposed revised blazar sequence, we show in figure 4, the density distribution of the logarithm of the spectroscopic redshift. *From* our data, the redshifts of FSRQs, and NLS1s are in the range: $0.021 < \log(1+z) < 0.62$, $0.03 < \log(1+z) < 0.68$ for NLS1s respectively while for

BLs, 0.016 < log (1+ z) < 0.46 for LSPs, 0.01 < log (1+ *z*) < 0.42 for ISPs and 0.11 < log (1+ *z*) < 0.47 for HSPs. From the data, we find that the average values of the redshift of these sources within the possible measurement error, follow the sequence BLs – FSRQs – NLS1s. We also observed from the data that NLS1s and FSRQs are located at higher redshifts relative to BLs. This agrees with the revised blazar sequence and the different stages of the cosmological evolution of these sources from young (BLs) → adult (FSRQs) → old (NLS1s). A parameter *t*-test and *K-S* test carried out on redshift data of NLS1s and blazar subtypes indicates that there is a fundamental difference between the underlying distributions of NLS1s, BLs and RQs in redshift. The cumulative probability function is shown in Figure 4 (b) while the result is shown in Table 1.

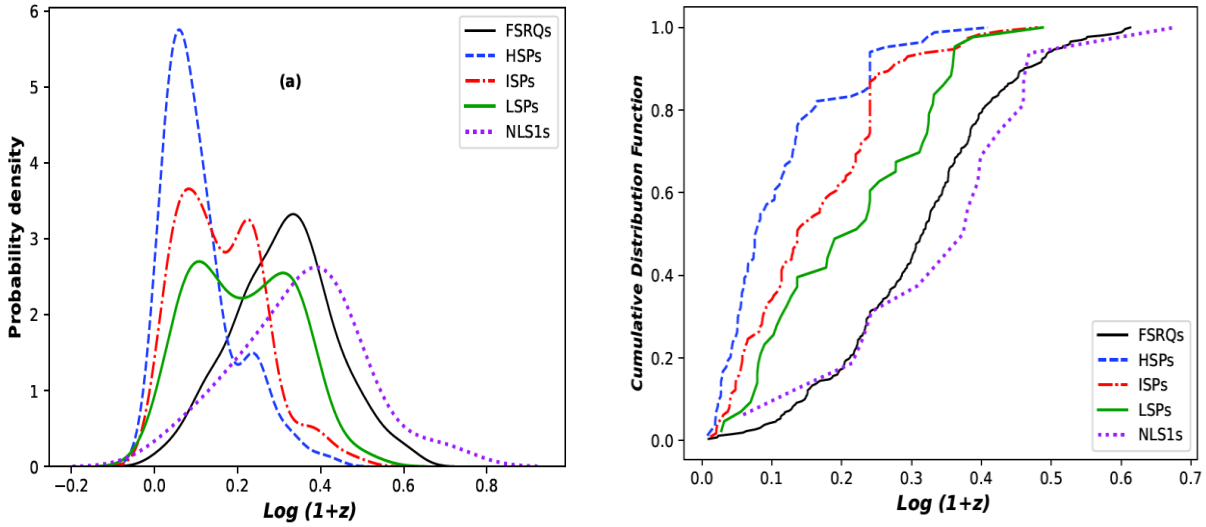

Figure 4: The density distribution of (a) spectroscopic redshift (b) cumulative distribution function of NLS1s, FSRQs and BLs

Table 1: The *K-S* test results of the parameters of NLSIs, FSRQs and BL Lac subclasses

Parameters	*Subsamples*	n_a	n_b	*d*	*p*
	NLS1s – HSPs	16	104	0.12	1.21×10^{-4}
	NLS1s – LSPs	16	88	0.38	3.01×10^{-5}
Logδ_γ	NLS1s - ISPs	16	52	0.21	2.90×10^{-6}
	NLS1s - FSRQs	16	263	0.26	1.03×10^{-6}
	NLS1s – HSPs	16	104	0.55	4.09×10^{-4}
	NLS1s – LSPs	16	88	0.25	1.22×10^{-6}
Log $L_{\gamma-ray}$	NLS1s - ISPs	16	52	0.38	1.83×10^{-6}
	NLS1s - FSRQs	16	263	0.37	2.81×10^{-6}
	NLS1s – HSPs	16	104	0.10	2.11×10^{-6}
Log *R*	NLS1s – LSPs	16	88	0.11	6.44×10^{-8}
	NLS1s - ISPs	16	52	0.10	2.19×10^{-6}
	NLS1s - FSRQs	16	263	0.11	2.00×10^{-7}
	NLS1s – HSPs	16	104	0.49	3.93×10^{-9}
	NLS1s – LSPs	16	88	0.31	1.82×10^{-7}
Log (1+z)	NLS1s - ISPs	16	52	0.28	2.89×10^{-9}
	NLS1s - FSRQs	16	263	0.14	3.07×10^{-5}

Correlations among the jetted AGNs Parameters

Whether or not the relativistic beaming properties of NLS1s, FSRQs, and BLs are intrinsically correlated is investigated in this section. The analysis of our data using Pearson's correlation theory can provide valuable information about the relationship between these parameters. In applying the statistical test, the degree of any obvious correlation is calculated using the product-

moment correlation coefficient r (Fisher, 1944; Press, 1992), defined as

$$r = \frac{\sum_{i=1}^{N}(X_i-\bar{X})(Y_i-\bar{Y})}{\sqrt{\sum_{i=1}^{N}(X_i-\bar{X})^2 \sum_{i=1}^{N}(Y_i-\bar{Y})^2}} \quad (8)$$

where X_i and Y_i are a pair of the logarithmic values of the parameters of our sample. We took the logarithmic values of the parameters in order to linearize any power-law relation and avoid the clustering of values. The presence or absence of any correlation will provide insight into the revised blazar sequence. The relation between the γ-ray Luminosity and γ-ray Doppler factor is shown in the scatter plot in figure 5. Interestingly, the revised blazar sequence is well prominent in the figure, with NLS1s occupying the upper right regime, BLs are located at the bottom left corner while FSRQs bridge the gap between them. Possibly, this is as expected in the relativistic beaming hypothesis such that the γ-ray emissions from the jets of NLS1s are presumably enhanced by relativistic Doppler boosting at small orientation angles to the line of sight. This distinct trend agrees with the prediction of the revised blazar sequence. We performed a regression analysis on individual and whole sample. The result is shown in Table 2 where a, c and r are the slope, intercept and correlation coefficient and their measurement error respectively while p is the value of the chance probability. The significance of the correlation is that similar effects are responsible for variations in the properties of NLS1s, FSRQs and BLs, which agrees with the prediction of blazar unified scheme via relativistic beaming.

Table 2: Results of the regression analysis for the individual and combined sample

plot	**Subsamples**	***a***	***Δa***	***c***	***Δc***	*r*	***chance probability***
$log\ L_\gamma$ $-\ log\ \delta_{\gamma-ray}$	Combined sample	4.25	0.50	43.54	0.50	0.78	2.44×10^{-7}
	FSRQs	2.67	0.30	42.83	0.70	0.63	1.02×10^{-4}
	LSPs	2.52	0.40	44.26	0.80	0.62	5.23×10^{-5}
	HSPs	2.43	0.30	43.69	0.70	0.59	3.43×10^{-5}
	ISPs	2.39	0.60	42.34	0.50	0.58	9.14×10^{-4}
	NLS1s	2.63	0.50	43.48	0.60	0.51	4.0×10^{-4}

Meanwhile, to investigate relativistic beaming effect on γ-ray properties of NLS1s, BLs and FSRQs. Fig. 5b shows the scatter plot of γ-ray Luminosity as a function of radio core-dominance. The NLS1s, BLs and FSRQs data tend to show a positive trend on the $L_\gamma - R$ plane. Regression analysis of the data give $r \sim 0.30$ for the combined sample. It can be argued that the observed positive trend implies that γ-ray emission in NLS1s, BLs and FSRQs is also beamed. Though, this positive trend exists only for the combined sample, it is discernible for individual subsamples. This implies that relativistic beaming alone cannot explain the variations in γ-ray emission of NLS1s, BLs and FSRQs.

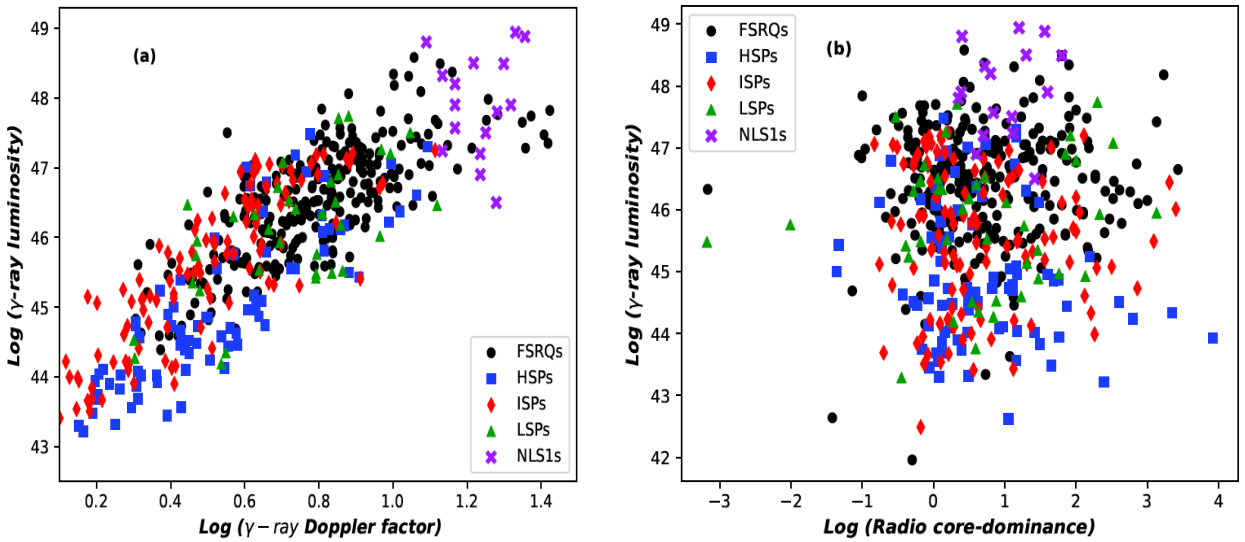

Figure 5: Relation between γ-ray Luminosity against (a) γ-ray Doppler factor (b) radio core-dominance on logarithmic scales for NLS1s, FSRQs and BLs

Furthermore, it is known that considerable uncertainties characterize the statistical analyses of data sample (Iyida et al. 2022a). Thus, in view of the extent of uncertainties in the γ-ray luminosity and γ-ray Doppler factor of NLSIs and blazar subclasses, we theorize that a more unbiased investigation of the revised blazar sequence requires the use of the average values of the parameters obtained from carefully chosen bins. The bining was done over the γ-ray *luminosity and* γ-ray Doppler factor as follows: $\delta_\gamma \leq 0.20$; $0.20 < \delta_\gamma \leq 0.40$; $0.40 < \delta_\gamma \leq 0.60$; $0.60 < \delta_\gamma \leq 0.80$; $0.80 \ \delta_\gamma \leq 1.00$; $1.00 < \delta_\gamma \leq 1.20$ and $1.20 < \delta_\gamma \leq 1.40$. The average value of $log\ L_\gamma - log\ \delta_{\gamma-ray}$ was calculated for each bin. The standard error of the average values was also calculated. The plot of the average values of $log\ L_\gamma - log\ \delta_{\gamma-ray}$ is shown in Figure 6. Clearly, NLS1s represent a sample of intrinsically higher γ-ray Doppler factor sources than their blazar counterparts, with average values higher by approximately 5 orders of magnitude. Linear regression analysis of$log\ L_\gamma - log\ \delta_{\gamma-ray}$ data gives a correlation coefficient $r \sim 0.76$. The correlation is found to be statistically significant at 98% confidence level and suggests that the level of relativistic beaming in NLS1s and Blazar subclasses which is consistent with the unification scheme via blazar sequence.

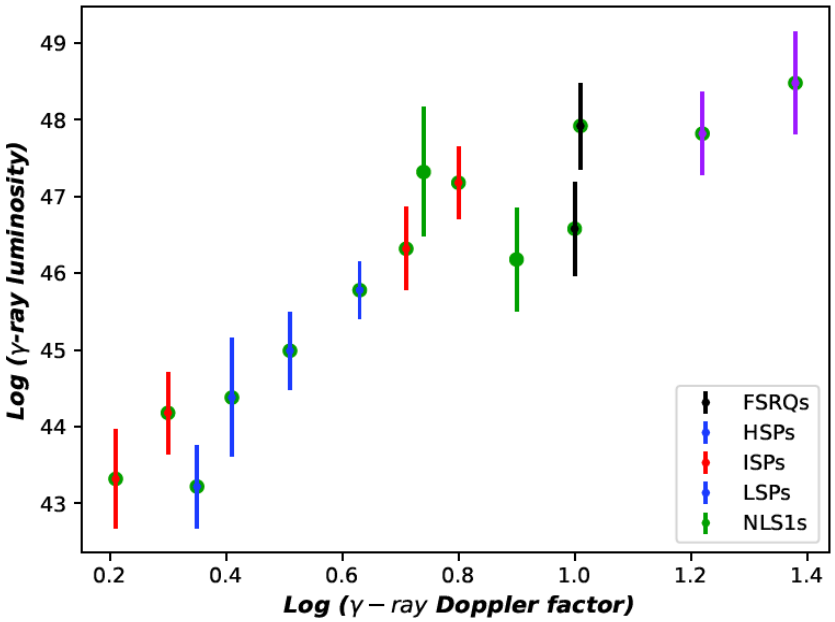

Figure 6: Relation between the average values of γ-ray luminosity and the binned γ-ray Doppler factor for NLS1s, FSRQs and BLs

The $\delta_\gamma - z$ and $\delta_\gamma - R$ Relations

A redshift-dependent luminosity of jetted AGNs of the form $L_\gamma = 4\pi\ d_L^2\ \frac{S}{(1+z)^{2-\Gamma\gamma}}$has been used to explain the blazar unification scheme and also as observed from equation (6), the γ-ray Doppler factor is somewhat redshift dependent, Thus, we examined the implications of this redshift effect of the present sample in a considerable detail and the uncertainties in the values equally taken care of by using $\delta_\gamma - z$ and $\delta_\gamma - R$ relations. The $\delta_\gamma - z$plot on logarithmic scales for the individual and combined sample is shown in Figure 7. It is observed that there is a sharp change in $\delta_\gamma - z$plot around $z \sim 0.60$. While majority of BLs are located at low z < 0.60 redshift, a vast majority of FSRQs and NLS1s are located at high (z > 0.60) redshift. On the other hand, the transition from BLs subclass at low redshifts to FSRQs and NLS1s at high redshifts is smooth as expected in the revised blazar sequence. Nevertheless, the strong selection effects in which the slope is dominated by the data in the low $\delta_\gamma - z$ plane is quite obvious in the plot. Therefore, to demonstrate this further, the plot is truncated at z = 0.60, which is indicated with the red line in Fig. 7a. Regression analysis of the combined $\delta_\gamma - z$ data yields $log\ \ \delta_\gamma = 0.51 \pm 0.20\ \ log\ \ (1+z) + 0.08 \pm 0.03$ with $r \sim 0.59$ for z <0.60 and $log\ \ \delta_\gamma = 0.62 \pm 0.20\ log\ \ (1+z) + 0.23 \pm 0.20$ with $r \sim 0.43$ for $z \geq 0.60$. These correlation results are significant at 0.95 confidence level. Therefore, these results show that the observed strong $\delta_\gamma - z$ correlation is dominated by the low redshift data and suggest significant differences in the slopes between the low and high combined z-data and a much weaker for $\delta_\gamma - z$ correlation for those sources with z > 0.60. Similarly, Fig. 7b shows the plot of $\boldsymbol{\delta_\gamma -}$

R. There is no apparent trend in the plot with NLS1s sharing the same parameter space with blazar subclasses in radio core dominance with up to 3 orders of magnitude but different in the property of Doppler factor. Regression analysis of NLS1s, FSRQs, and BLs data show a very marginal correlation with coefficient $r \sim 0.23$ and 0.35 for NLS1s and combined blazar samples respectively.

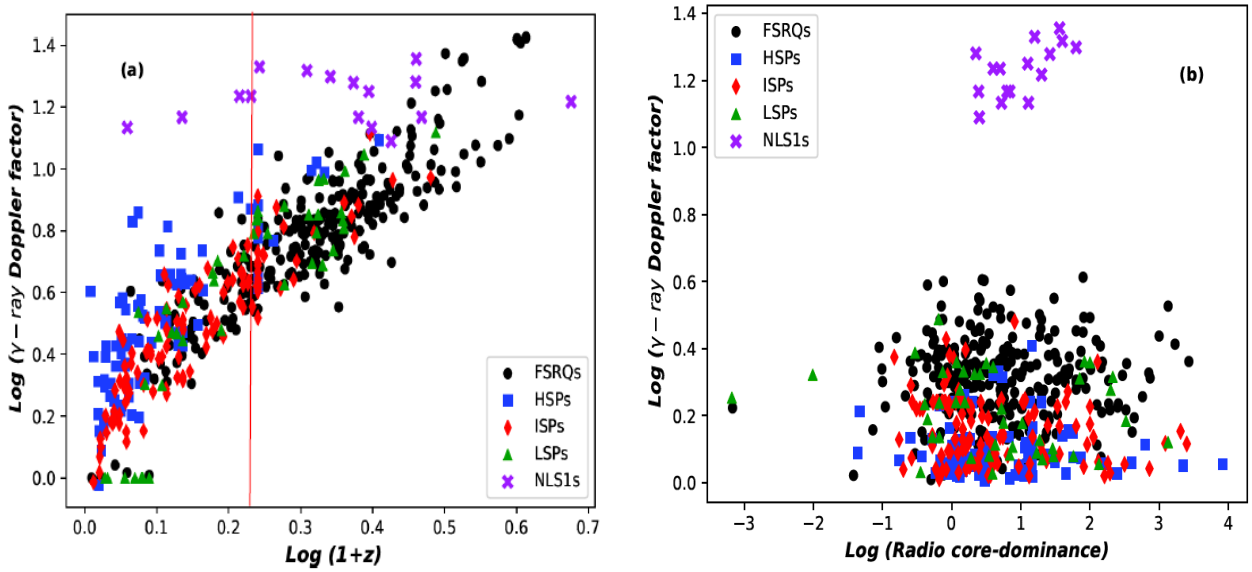

Figure 7: Scatter plot of δ_γ against (a) log (1 + z) (b) radio core dominance on Logarithmic scales for NLS1s, FSRQs and BLs

Discussion

The unified model of jetted AGNs proposes that different observational classes of these sources are a single type of physical object observed under different conditions. The idea of unification for different types of jetted AGNs came when it was realized that projection effects can play an important role in the interpretation of some of these sources. Since then, numerous efforts have been made in determining to what extent are jetted AGNs simply different manifestations of the same object viewed from different angles. The first attempt at unification of AGNs was made by Scheuer & Readhead, (1979) when they proposed that FSRQs are the beamed counterparts of radio-quiet quasars. Since then, several other attempts have been recorded leading to different unification schemes. The blazar sequence unification scheme proposes that both FSRQs and BL Lac objects are forms of objects with the same physical process but differ in bolometric luminosity (Fossati et al. 1997; 1998; Ghisellini et al. 1998; Abdo et al. 2010). The most prominent is the significant anti-correlation between ν_{peak} and synchrotron peak luminosities (L_{syn}) of the blazar subclasses. However, violation to this scheme has been established and findings of sources with powerful relativistic jets appear to break this simple scheme (Osterbrock and Pogge, 1985; Grupe 2000; Botte et al. 2004; Foschini 2011, 2014). The relativistic beaming model is a proposed theory used to explain certain observed properties of jetted AGNs and it is well-known and proven by rapid flux variability ranging from radio to high energy γ-ray bands (Kovalev, 2009). A simple significance of this model is that relativistic Doppler boosting and symmetrical projections effects are estimated to be prominent in blazar subclasses with small viewing angles to the line of sight of an observer. Though, the blazar sequence was originally introduced using few sources (Fossatti et al. 1998), it could not explicitly give credence to relativistic beaming, thus, we investigated this relativistic beaming effect in the context of the revised blazar sequence.

We show in our results that there is no fundamental difference in the shape of relativistic beaming indicators of NLS1s, FSRQs and BLs. It is generally known from the beaming model that FSRQs with larger values of γ-ray Doppler factor are strongly beamed than BLs. It is observed from figures 1, 2 and 3 that there is continuous distribution of both γ-ray Doppler factor, γ-ray luminosity and radio core-dominance parameter of NLS1s, FSRQs and BLs. The distributions parameters actually support the revised blazar sequence as there are clear divisions between the subclasses. In the blazar scenario, one would expect a continuous distribution from BLs to FSRQs. We observed from our results that NLS1s and FSRQs have high average values of radio core-dominance parameter and γ-ray Doppler factor, the sequence in which they appear is consistent with the

revised blazar sequence. Perhaps, the strongest γ-ray emission detected around NLS1s is an indication of the strong beaming effect, in which case, BLs and FSRQs may differ by orientation (Chen et al. 2016; Li et al. 2017)

Interestingly, in figures 5 and 6, we observed that the revised blazar sequence is well prominent with NLS1s occupying the upper right side while BLs are located at the bottom left corner with FSRQs bridging the gap between them. This distinct trend agrees with the prediction of the revised blazar sequence. Our results are not far from Chen at al. (2021) who found that the accretion rate of NLS1s is similar to FSRQs, which imply that relativistic electrons of the jet of FSRQs and NLS1s are fast cooling, thus, implying that NLS1s may belong to blazar sequence. The observed trend shown in our analysis for the NLS1s and blazar subtypes is suggestive that similar inherent physical processes operate in all the blazar subclasses. The trends of the γ-ray luminosity and γ-ray Doppler factor data increasing from BLs to NLS1s through FSRQs implies increasing high energy emission processes are responsible for the relativistic beaming effect. Thus, this suggests that relativistic beaming indicators are essential for understanding the properties of and the relationship between NLS1s and blazar subclasses.

Figure 7 shows the $\log \delta_\gamma - \log (1+z)$ for NLS1s, FSRQs, and BLs. The large scatter seen in the figure at low redshifts suggests that the selection effect is playing some role (Alhassan *et al.* 2013; Odo *et al.* 2014; Iyida et al. 2021). Obviously, the majority of BLs in the current sample are located at low redshifts ($z < 0.60$), implying that they are the least beamed while FSRQs and NLS1s with larger redshifts are more beamed. If this is actually the case, the sequence of variation of the γ-ray Doppler factor with the redshift may be an artifact of the selection effect at low and high redshifts. We observe from the figure that there is a steep change in the plot at $z \sim 0.60$. This indicates that there are distinct γ-ray Doppler factor values for our sample at different redshifts. Consequently, it can be estimated that, for a s mall sample with flux density parameters, sources with low redshifts ($z \leq 0.60$) will show a higher dependence on the luminosity as a function of redshift when compared to the high redshifts ($z > 0.60$) sources.

CONCLUSION

we have compared the beaming effects of NLS1s, and FSRQs in the context of revised blazar sequence. Our results show no dichotomy in the distributions of both γ-ray Doppler factor and core dominance parameter in such a way that is consistent with the revised blazar sequence. The observed properties of these NLS1s are comparable and consistent with the sequence NLS1s – FSRQs – BLs. This evolutionary sequence suggests that these jetted AGNs start at lowest redshifts as BLs and evolves into a NLS1s as the source ages through FSRQs. These sources are agreement with the relativistic beaming unification scheme for NLS1s and blazar subtypes.

ACKNOWLEDGEMENT

We thank an anonymous referee for insightful comments and constructive suggestions.

REFERENCES

Abdo, A. A., Ackermann, M., Ajello, M., Atwood, W.B., et al. Bright active galactic nuclei source list from the first three months of the *Fermi* LAT All-Sky Survey. *Astrophysical J*., 700: 597 (2009a)

Abdo, A.A., Ackermann, M., Ajello, M., et al. Fermi observations of TeV-selected active galactic nuclei 2009b, ApJ, 707, L142

Ackermann, M., Ajello, M., Allafort, A., Baldini, L. et al. Search for gamma-ray emission from X-ray-selected Seyfert galaxies with Fermi-LAT. Astrophysical Journal, 747:104-121, (2012)

Acero, F, Ackermann, M, Ajello, M, Albert, A, Atwood, W B. Fermi Large Area Telescope third source catalog. *Astrophysical J*. Suppl. 218, 23–64 (2015)

A. I. Audu, F. C. Odo, E. U. Iyida, O. Okike, & A. A. Ubachukwu. On the Unified Scheme of γ-ray Emitting Jetted Active Galactic Nuclei. Astrophysics, 66; 2 (2023)

Berton, M., et al.: Radio-emitting narrow-line Seyfert 1 galaxies in the JVLA perspective Astron. Astrophys. 614, A87 (2018)

Bai, J. M. and Lee, M. G., 2001. New evidence for the unified scheme of BL Lacertae objects and fr i radio galaxies *Astrophys. J*. 548, 244

Bicknell, G. V. 1995, Spectral signatures of fast shocks. II. Optical diagnostic diagrams *Astro. Physical Journal Supple*., 101, 29

Chen YY, Zhang X, Xiong DR, Wang SJ, Yu XL. 2016. The beaming effect and γ-ray emission for Fermi blazars. Res. Astron. & Astrophys. 16: 13-23

Chen, Y. Y., & Gu, Q. S. 2019, The black hole mass, jet power and accretion in blazars and flat-spectrum radio-loud narrow-line Seyfert 1 galaxies Ap&SS, 364, 123

Chen, Y. Y., & Gu, Q. S. et al. (2021) From the Fermi Blazar Sequence to the Relation between Fermi Blazars

and γ-Ray Narrow-line Seyfert 1 Galaxies. *Astrophysical Journal*, 906:108

Iyida, E.U. Eya, I.O. & Odo, F.C. On the unified view of extragalactic sources based on their broadband emission properties. J. Astrophys. Astron., 42, 107 (2021)

Iyida, E.U., Odo, F.C. Chukwude, A.E. & Ubachukwu, A.A.: Multi-frequency study of spectral indices of BL Lacertae objects and flat-spectrum radio quasars NewA, 90, 101666, (2022a)

Iyida, E.U., Eze, C.I. & Odo, F.C. On the Evolution of Seyfert galaxies, BL Lacertae objects and Flat-spectrum radio quasars. **Astrophysics and Space Science**. 367, 11 (2022b)

Fan, J, Liu, Y., Yang, J., Lin, C., Hao, J. et al. 2016, Observing black holes spin *Galaxies*, 4, 16

Fisher, R. A. 1944, Statistical Methods for Research Workers (Edinburgh Oliver & Boyd)

Foschini L. What we talk about when we talk about blazars. Front. Astron. Space Sci. 4, 6 (2017)

Foschini, L., Lister, M. Antón, S. et al. A new sample of gamma-ray emitting jetted active galactic nuclei—preliminary results, Universe, 7, 37, (2021).

Fossati, G., Celloti, A., Ghisellini, G., Maraschi, L., 1997, *Mon. Not. R. Astron. Soc.*, 289, 136

Fossati, G., Maraschi, L., Celotti, A. et al., 1998. *Mon. Not. R. Astron. Soc*. 299:433

Ghisellini, G., Celotti, A., Fossati, G., et al., 1998, *Mon. Not. R. Astron. Soc*, 301, 451

Ghisellini, G, Righi, C., Costamante, L., Tavecchio, F., 2017. *Mon. Not. R. Astro. Soc.* 234, 23-34

Giommi, P., et al., 2012, Astro. & Astro., ,541, A160

Gupta, A. C. 2011, *Journal of Astrophys. Astron.*, 32, 155

Kang, S.-J., Chen, L., & Wu, Q. 2014, Constraints on the minimum electron Lorentz factor and matter content of Jets for a sample of bright *Fermi* blazars ApJS, 215, 5

Kellermann K. I., Sramek R., Schmidt M., et al., 1989, *Astro. Journal*, 98, 1195

Lister, M.L. Aller, M., Aller, H. Hovatta, T. *et al.* 2011, *Astroph. Journal*, 742, 27

Lister, M.L. Aller, M., Aller, Aller, H.D. *et al.* 2013, *Astronomical Journal. 146(5), 120* 27

Mao, P., Urry, C. M., Massaro, F., Paggi, A., Joe, C. et al., 2016, *Astroph. Journal, Supp*., 224, 26

Mattox, J. R., Bertsch, D. L., Chiang, J., *et al.* 1993. *Astroph. Journal*. 410, 609

Meyer, E. T., Fossati, G., Georganopoulos, M., Lister, M. L.,2011, *Astrophys. Journal.*, 740, 98

Murphy, D.W., Brown, I.W., Perley, R.A. 1993, *Mon. Not. R. Astron. Soc*. 264, 298

Nalewajko, K. 2013, The brightest gamma-ray flares of blazars. MNRAS, 430, 1324

Nieppola, E., Volatoja, E., Tornikoski, M. et al., 2008, Astro. & Astrop. 488, 867-872

Osterbrock, D., & Pogge, R.W., 1985, Narrow-line Seyfert 1s: 15 years later. ApJ, 297, 166

Orr M. J. L., Browne I. W. A., 1982, *Mon. Not. R. Astron. Soc*., 200, 1067

Padovani, P., Perlman, E.S., Landt, H. et al., 2003, What types of jets does Nature make? A new population of radio quasars *Astrophysical Journal.*, ,588, 128 https://iopscience.iop.org/article/10.1086/373899/meta

Padovani, P., Giommi, P., Rau, A., 2012, The discovery of high-power high synchrotron peak blazars *Mon. Not. R. Astron. Soc*., 422, L48

Paliya, V. S., Stalin, C. S., Shukla, A., & Sahayanathan, S. The Nature of γ-Ray Loud Narrow-line Seyfert I Galaxies PKS 1502+ 036 and PKS 2004− 447. 2013, ApJ, 768, 52

Pei Z., Fan J., Bastieri D., Yang J., Xiao H., Radio core dominance of Fermi/LAT-detected AGNs. 2020a, Sci. China Physics, Mech. and Astro., 63, 25951

Pei, Z., Fan, J., Yang, J., et al. The estimation of γ-ray Doppler factor for Fermi/LAT-detected blazars publications of the Astronomical Society of Australia (2020b), 37, e043,

Perlman, E., Stocke, J. T. 1996. The EINSTEIN slew survey sample of BL Lacertae objects. *Astrophys. Journal.*, 406, 430.

Press WH, Teukolsky SA, Vetterling WT, Flannery BP, Numerical Recipes in Fortran: The Art of Scientific Computing (Cambridge University Press, Cambridge, UK, 1994).

Scheuer, P.A.G., Readhead, A.C.S. 1979. Superluminally expanding radio sources and the radio-quiet QSOs *Nature.* 277, 182

Sun, X.N., Zhang, J., Lin, D.B., Xue, Z.W., Liang, E.W., Zhang, S.N. Jet properties of GeV-selected radio-loud narrow-line Seyfert 1 galaxies and possible connection to their disk and corona Astrophys. J. 798, 43 (2015)

Sun, X.N., Zhang, J., Lu, Y., Liang, E.W., Zhang, S.N. Spectral Variation of NLS1 Galaxy PMN J0948+ 0022 J. Astrophys. Astron. (2014)

Urry C. M., Padovani P. Unified Schemes for Radio-Loud Active Galactic NuREFERclei. Publications Astron Soc Pacific 107: 803-845 (1995).

Wu, Z. Z., Gu, M. F., & Jiang, D. R. 2009, The debeamed luminosity, synchrotron peak frequency and black hole mass of BL Lac objects *Res. Astron. Astrophys.* 9,168

Zhang, J., Zhang, S.-N., & Liang, E.-W. 2013, Blazar anti-sequence of spectral variation within individual blazars: Cases for Mrk 501 and 3C 279. ApJ, 767, 8

Zhang, J., Xue, Z.-W., He, J.-J., Liang, E.-W., & Zhang, S.-N. 2015, Correlations among the Jet, accretion disk, and Broad-Line Region of flat Spectrum Radio Quasars ApJ, 807, 51